Photophysical Processes in the Complexes of DNA with Ethidium Bromide and Acridine Orange: A Femtosecond Study

ARTICLE *in* THE JOURNAL OF PHYSICAL CHEMISTRY B · JANUARY 2001

Impact Factor: 3.3 · DOI: 10.1021/jp002615o

4 AUTHORS:

Alexei Kononov
Saint Petersburg State University
29 PUBLICATIONS **192** CITATIONS
SEE PROFILE

Evgenia Borisovna Moroshkina
Saint Petersburg State University
22 PUBLICATIONS **82** CITATIONS
SEE PROFILE

Nikolai Tkachenko
Tampere University of Technology
267 PUBLICATIONS **4,561** CITATIONS
SEE PROFILE

Helge Lemmetyinen
Tampere University of Technology
422 PUBLICATIONS **6,393** CITATIONS
SEE PROFILE

Photophysical Processes in the Complexes of DNA with Ethidium Bromide and Acridine Orange: A Femtosecond Study

Alexei I. Kononov* and Evgeniya B. Moroshkina

Institute of Physics, St. Petersburg State University, Ulyanovskaya 1, 198904 St. Petersburg, Russia

Nikolai V. Tkachenko* and Helge Lemmetyinen

Institute of Materials Chemistry, Tampere University of Technology, PL 541, 33101 Tampere, Finland

Received: July 24, 2000; In Final Form: October 16, 2000

Ethidium bromide (EB) and acridine orange (AO) in the complexes with DNA in aqueous solution were studied using variety of spectroscopy techniques: emission up-conversion, absorption pump−probe, flash-photolysis, steady-state luminescence, and circular dichroism (CD). Combination of the methods allowed to detect oxidized form of ethidium and to associate this with a fast 10 ps component observed in the up-conversion experiments. Thus, a photoinduced electron transfer from a small fraction of the dyes to the DNA bases was concluded. It suggests that those DNA sites have a redox potential higher than −0.9 V (an upper limit for the excited-state oxidation potential of ethidium), while the redox potential of the most affinic DNA bases, thymine and cytosine in water, is −1.09 V. It is proposed that certain conformations of the stacked bases have low-lying electronic orbitals. The involvement of such low-lying electronic levels in the processes of electron transfer through DNA stack is suggested. The results obtained by the pump−probe experiments for the AO−DNA system and by the CD measurements for the EB−DNA complex point at a delocalization of the electronic excitation over the neighboring dyes separated by two base pairs, i.e., 10 Å, in the DNA stack.

Introduction

Synthetic dyes intercalating into DNA double strand are widely used as a tool to study the process of photoinduced charge transfer through the DNA stack. In the past years, a significant progress was achieved in this field.[1] First, an oxidative damage of the bases at the distance of about 40−200 Å was observed.[2,3] And vice versa, the distant repairing of the thymine dimer appeared to be possible.[4] What is more interesting, the efficiency of the reactions exhibited shallow distance dependence.[2−4] Such processes involved electron transfer from the remote site to the excited metal complexes[2,4] or anthraquinone molecules[3] linked to duplex DNA. To explain a weak distance dependence, two mechanisms are considered: charge hopping[1b,c] and a strong electronic coupling between the bases that leads to semiconductor properties, the charge being delocalized over the bases.[1b] A polaron-like mechanism was also proposed.[3b] The model of charge hopping between the guanine bases has been experimentally supported in the study of sequence dependence of charge transfer from guanine radical cation through the duplexes.[5] It seems, however, that this model cannot explain a very efficient long-range photooxidation process recently observed in some duplex structures.[3b,6] It also cannot be applied when the excited intercalator serves as a donor and another intercalator serves as an acceptor. An efficient electron transfer was observed in the studies of 15 base pair DNA duplex tethered with metallointercalators[7] and of ethidium-modified duplexes of various lengths.[8] It was shown[8] that DNA-mediated electron transfer from the excited ethidium to a metallointercalator depended only weakly on the donor−acceptor separation. From that study,[8] it also followed that the electron transfer over more than 10 Å occurred in a picosecond time scale. Similar observations were reported earlier for the complexes of DNA with metallointercalators nonfixed covalently.[9] It should be noted, however, that those results could be explained by "clustering" of metallocomplexes.[10] However, the results obtained on the duplexes of fixed length, tethered with ethidium and rhodium intercalators,[8] cannot be explained by "clustering". They are clearly in contrast with the results obtained in similar systems.[11] Brun and Harriman, who studied photoinduced electron transfer between ethidium bromide (EB), acridine orange (AO) and *N*,*N*′-dimethyl-2,7-diazapyrenium, stated that the distance dependence of the rate was exponential and the process occurred on nanosecond time scale.[11a] Later, it was shown that those results agree well with the theoretical analysis based upon quantum chemical calculations of DNA-mediated donor−acceptor interactions that included contributions from every single pathway linking donor and acceptor.[12]

Scheme 1 illustrates the redox properties of the intercalators used in the studies of Barton et al.[7−9] along with that of the DNA bases.[13] In principle, the process of electron transfer through DNA in the absence of intermediates, as it takes place in those systems, falls into the pattern of electron tunneling that is strongly distance dependent.[14] On the other hand, if the energy difference between the bridge, donor, and acceptor orbitals is small, the theory predicts complex distance behavior.[15] In the studies of Kononov and Bukina,[16] it was shown that in stacked adenines there are electronic levels lowered by about 1 eV compared to free bases in solution. Those low-lying electronic orbitals (shown in Scheme 1 as dashed line) would contribute

* Corresponding authors. E-mail: kononov@snoopy.phys.spbu.ru, nikolai.tkachenko@tut.fi.

10.1021/jp002615o CCC: $20.00
Published on Web 12/20/2000

SCHEME 1: Energetic Levels of the Donor−DNA−Acceptor System Used in the Studies of Barton et al.[7−9] [a]

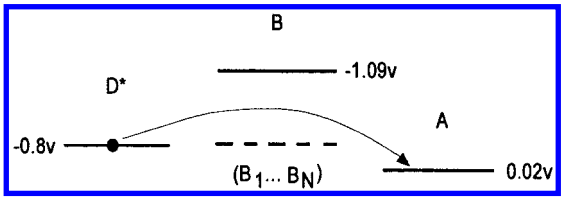

[a] Donor (D*)−excited ruthenium metallointercalator with the redox potential $E(D^*/D^+) = -0.8$ V or excited EB (the oxidation is irreversible, the values reported[8,11a] for $E(D^*/D^+)$ −0.52 V and ∼−0.9 V). Acceptor (A)−rhodium metallointercalator with $E(A/A^-) = 0.02$ V. B = nucleic acid cytosine or thymine bases with $E(B/B^-) = -1.09$ V in aqueous solution.[13] $B_1 \cdots B_n$ = stacked bases with low-lying electronic states (see text). Potentials are given vs NHE.

significantly to the total donor−acceptor electronic coupling. If such levels are realized in DNA, electron transfer from the excited dyes to DNA bases might manifest itself as a fast component in the fluorescence decay of the intercalator. That idea was the starting point in our study. Along this, our concern was the excitation dynamics over molecules intercalated into DNA. That might compete with the processes of electron-transfer being under the study. Traditionally, it implies energy transfer of Förster type.[17] Fluorescence polarization studies clearly indicate that such a process takes place indeed.[18] In addition, circular dichroism (CD) studies of the DNA−dye systems reveal a perturbation of the spectra with increasing of the binding ratio,[19] which is supposed to be due to degenerative excitonic coupling, in other words, energy delocalization over neighboring dyes. However, CD spectra cannot be easily interpreted. Here we use another tool for probing the energy delocalization, namely, the transient absorption studies.

In this work, we have studied the behavior of EB and AO (classic intercalators) in the excited state in solution and in the complexes with DNA in relation to the binding ratio over the time range from microsecond to femtosecond. We have observed a fast component of about 10 ps in the fluorescence decay of the complexes of the intercalators with DNA. This is proposed to be due to an electron transfer from the excited intercalator to low-lying states of DNA bases. The corresponding absorption spectrum of the oxidized EB has been observed in flash photolysis study of the EB−DNA system. The involvement of such low-lying electronic levels in the processes of electron transfer through DNA stack is suggested. Strong bleaching of the ground-state absorption of the AO−DNA complex compared to AO solution, as observed in the pump−probe experiments, has been explained in terms of electronic energy delocalization over the dyes intercalated into the DNA stack. For the EB case, such conclusion stems from the results of the CD measurements performed in this work.

Experimental Section

Sample Preparation. Calf-thymus DNA, ethidium bromide, and acridine orange were obtained from Sigma and used as received. Solutions were prepared in water purified using Millipore Milli-Q system and containing 5 mM sodium chloride and 0.1 mM tris or phosphate buffer. Concentration of DNA per nucleotide phosphate was typically 1 mM and determined by the absorption spectroscopy using the extinction coefficient of 6600 M^{-1} cm^{-1} at 260 nm. In femtosecond measurements the DNA concentration was about 2 mM and no buffer was added. A small amount of stock solutions of the dyes was added to DNA solution followed by shaking for an hour. The amount of bound dye was calculated using the following equation:

$$C_B = \frac{\epsilon_f^\lambda C_T - A^\lambda/l}{\epsilon_f^\lambda - \epsilon_b^\lambda} \quad (1)$$

where C_B is the concentration of bound dye, C_T is the total amount of the dye present, l is the cell path length, A^λ is the optical density at wavelength λ, and ϵ_f^λ and ϵ_b^λ are the extinction coefficients for the free and bound dye, respectively. The following extinction coefficients were employed: $\epsilon_{(EB,\ 484)} = 5.7 \times 10^3$ M^{-1} cm^{-1}, and $\epsilon_{(AO,\ 492)} = 5.7 \times 10^4$ M^{-1} cm^{-1} in aqueous solution. All experiments were done on air-equilibrated solutions at 20 ± 3 °C.

Spectral Measurements. UV−vis absorption measurements were made with a Shimadzu UV-2501 PC spectrophotometer. CD spectra were recorded with a Jóbin-Ivòn spectropolarimeter. The circular dichroism was expressed as $\Delta\epsilon = \epsilon_l - \epsilon_r$, the difference in extinctions coefficients for left- and right-circularly polarized light for 1 mol of bound EB. Luminescence spectra were recorded on a Fluorolog 3 spectrofluorimeter (Spex Inc.). Quantitative measurements were made on a Hitachi 850 spectrofluorimeter using 1 cm path cell. The luminescence intensities were corrected for inner filter effect.

Time-Resolved Measurements. Fluorescence decay profiles were measured using the time-correlated single-photon-counting (TCSPC) technique with the instrument described elsewhere.[20a] The excitation wavelength was set to 570 nm. In some cases the dye laser pulses were frequency doubled and the excitation wavelength was 305 nm. The decays were collected until 5000−10 000 counts accumulated in the highest channel. Data fitting was made after deconvolution with the instrument response function (fwhm = 60 ps) by a least-squares method using in-house software.

Flash photolysis studies were made with a Q-switched frequency-doubled Nd:YAG laser (532 nm, 20 ns pulse, 30 mJ). A pulsed Xe arc lamp was used as a monitoring beam. The angle between exciting and monitoring beams was about 30°. Solutions had an absorbance in 2 mm cell less than 0.2 at the excitation wavelength. "In-pulse" transient absorption spectra were recorded point-by-point with 5−50 individual records being computer-averaged at each wavelength. Absorbance difference spectra of the transient species on microsecond time scale were obtained by three-exponential fitting of all individual data traces at a given wavelength simultaneously. In-house software was used.

Femtosecond Measurements. The setup used in the femtosecond pump−probe and fluorescence up-conversion measurements was described previously.[20b] Briefly, a Ti:sapphire laser (TiF50, CDP-Avesta, Moscow, Russia) pumped by an Ar ion laser (Innova 316, Coherent) generated pulses (100 fs, 800 nm) at 80 MHz repetition rate. In emission up-conversion experiments the pulses were frequency doubled, and thus excitation wavelength was 400 nm and excitation density ∼0.05 mJ/cm^2. The time resolution was ∼150 fs as determined from the cross-correlation function. In absorption pump−probe experiments the base pulses were amplified using multipass Ti:sapphire amplifier (CDP-Avesta, Moscow, Russia) pumped by a second harmonic of the LF114 Nd:YAG Q-switched laser (Solar TII, Minsk, Belorussia) operating at repetition rate of 10 Hz. The pump pulses were frequently doubled providing ∼10 mJ/cm^2 excitation density (a spot diameter ∼40 μm) at 400 nm. The probe beam was focused into a cell with water to generate a white light continuum. The white light pulses were collimated

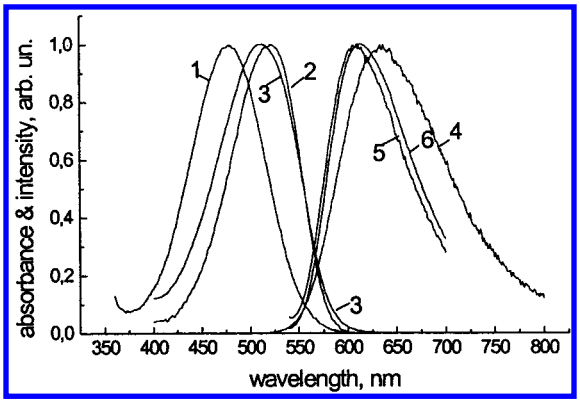

Figure 1. Absorption spectra: EB in aqueous solution (1); EB−DNA, $r = 0.18$ (2), $r = 0.48$ (3). Fluorescence spectra: EB in aqueous solution, $\lambda_{ex} = 500$ nm (4); EB−DNA, $r = 0.05$ (5), $r = 0.48$ (6), $\lambda_{ex} = 530$ nm.

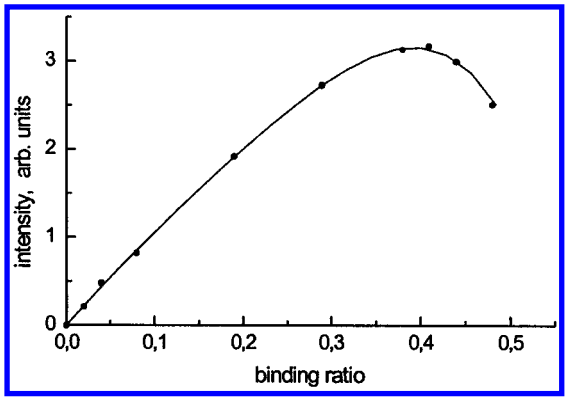

Figure 2. Binding ratio dependence of the integral fluorescence intensity of EB−DNA solution, $\lambda_{ex} = 570$ nm.

TABLE 1: TCSPC Measurements of EB−DNA System at Various *r* and EB in Water ($\lambda_{ex} = 570$ nm)

r	τ (ns)	*r*	τ (ns)
0.02	21.7	0.45[a]	14.7 (87%)
0.04	21.7		0.9 (13%)
0.1	21.7	0.5[a]	11.6 (52%)
0.2	21.3		2.2 (33%)
0.35	20.2		0.36 (15%)
0.4	18.7	EB	1.62

[a] $\lambda_{ex} = 303$ nm; accuracy of τ − 3% for major components.

TABLE 2: TCSPC Measurements of AO−DNA System and AO in Water

r	τ (ns)
0.1	5.0
0.4	4.75 (62%) 1.2 (19%) 0.15 (19%)
AO	1.84

$\lambda_{ex} = 303$ nm, accuracy of τ − 3% for major components.

and divided into parts. One part served as the reference and another as the probe. The instrument allowed one to record transient spectra in with time resolution better than 150 fs. Usually, averaging of 100 pulses was used to improve the signal-to-noise ratio. The spectra were recorded with progressively increased delay time starting with 100 fs steps. Thus, the obtained data were fitted globally using multiexponential model. The fitting routine provides also compensation of the group velocity dispersion of the probe pulse and convolution with the instrument response function. In both cases of up-conversion and pump−probe experiments the samples were placed in a 1 mm quartz rotating cuvette.

Results

EB is a classic strong intercalator with a binding constant $K = 2.6 \times 10^6$ M^{-1} and a saturation (number of available binding sites) $n = 0.5$/base pair.[21] Photophysics of EB−DNA complexes were extensively studied from nanosecond to millisecond time scale.[22,23] When this paper was in preparation, a femtosecond study of EB in water and in the complexes with nucleotides was published.[24]

Figure 1 shows the absorption and luminescence spectra of EB in water solution and of its complex with DNA. With increasing binding ratio (*r*, number of bound dye molecules per base pair), the fluorescence spectrum of EB is slightly shifted from 610 nm (curve 5) to 616 nm (curve 6). A small red tail in the absorption (curve 3 compared to curve 2) is also observed. Note that those changes cannot be explained by a contribution of the free dye to the spectra. The dependence of the integral of steady-state fluorescence intensity (*I*) on *r* is shown in Figure 2. It is seen that the plot has a nonlinear dependence on *r*, suggesting that the quenching efficiency of the EB molecules increases at high vales of *r*. A similar dependence was observed for the fluorescence lifetimes. It is known that the fluorescence lifetime (τ) of the intercalated EB is 21−23 ns.[11a,22] We have obtained $\tau = 21.7 \pm 0.5$ ns for low dye/DNA binding ratio. However, at $r > 0.2$, τ decreases noticeably, as indicated in Table 1. At $r > 0.4$, the decay profile becomes complex showing several components in nanosecond time scale. The weak component with lifetime of 1−2 ns can be assigned to the free dye, since the lifetime of EB in aqueous solution is 1.6 ns.[25] The AO−DNA system ($K = 2 \times 10^6$ M^{-1} and $n = 0.5$/base pair[26]) also reveals a complex fluorescence decay behavior at $r > 0.4$ (see Table 2), while at low *r* the AO−DNA solution exhibits single-exponential decay with $\tau = 5.0$ ns as observed earlier.[11a,27] The component with $\tau = 1.2$ ns can be attributed to the nonbound (or surface-bound) AO molecules. A similar lifetime was obtained for AO in water[27] (we have obtained somewhat longer $\tau = 1.8$ ns).

The fluorescence decay of EB and AO take place not only in nanosecond time domain, but it was observed also in picosecond time scale using the fluorescence up-conversion method. Figure 3 presents the fluorescence decay curves for EB−DNA at various *r*. They reveal a fast component of about 10 ps which becomes evident at $r = 0.3$ and decreases with increasing *r*. The results of two-exponential fitting are presented in Table 3 (second component in all cases is practically constant on the time scale used). The relative amplitude of the component at $r = 0.3$ is 65% (Figure 3b). Note that excitation wavelength is 400 nm, and the emission quantum yield (φ) of EB−DNA solution excited at this wavelength appears to be two times smaller than that of EB−DNA solution excited at 350 and 570 nm suggesting heterogeneity of the EB−DNA system.

The major decay component of the EB−DNA complexes at wavelengths close to the fluorescence band maximum is almost independent of the wavelength (Figure 3b). This component cannot be attributed to the dynamic Stokes shift (Franck−Condon thermalization, solvent reorganization dynamics). Dynamic Stokes shift can be observed at shorter wavelengths (580 nm, Figure 4 (upper)) as a short-lived component (~0.6 ps). For comparison, the decay curves for EB in aqueous solution are also shown in Figure 4 (bottom). When recorded at 610 nm, the decay curve exhibits a fast component that is obviously related to the dynamic Stokes shift. The exponential fit gives the value of about 1 ps for this component. The same value of 1 ps has recently been obtained in the study of Barton et al.[24]

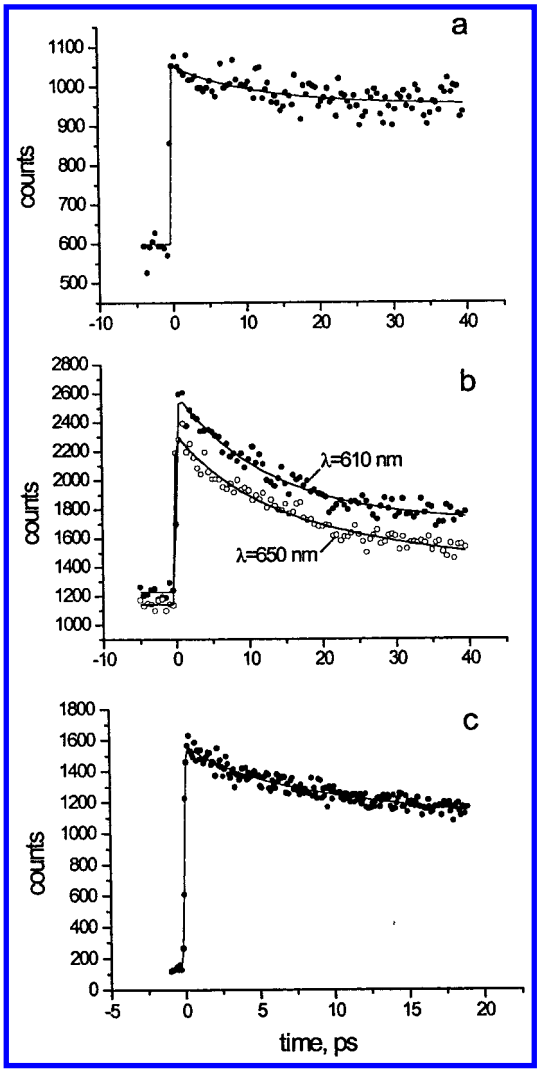

Figure 3. Fluorescence decays of EB−DNA: (a) $r = 0.1$, $\lambda_{em} = 610$ nm; (b) $r = 0.3$, $\lambda_{em} = 610$ and 650 nm; (c) $r = 0.5$, $\lambda_{em} = 650$ nm.

TABLE 3: Lifetimes and Fractional Amplitudes (*A*) of the Fast Components Obtained through Two-Exponential Fitting of the Decay Curves Recorded in Picosecond Time-Domain Using the Up-Conversion Method for EB−DNA System at Various Binding Ratios[a]

r	τ (ps)	A (%)	r	τ (ps)	A (%)
0.1	12 ± 5	22 ± 5	0.45	9 ± 2	51 ± 2
0.3	13 ± 2	65 ± 3	0.5	11 ± 2	32 ± 2

[a] The slow components are practically constant within the time scales used.

The fluorescence decays of AO−DNA complex also reveal a component with lifetime of 5−10 ps, which becomes stronger at higher r (shown in Figure 5). Absorption spectra of the AO in the aqueous solution indicate strong aggregation of the dye. Therefore, it was impossible to compare the results of studies of AO in H_2O with that of the AO−DNA system. We suppose, however, that the fast decay observed for AO−DNA in water is a characteristic feature of the intercalated AO molecules, and their fluorescence quenching takes place mainly in the picosecond time scale.

The photochemistry of the EB−DNA system in nanosecond and longer time domains was studied using the flash photolysis method. It allows us to reveal the nature of the fluorescence quenching observed. The transient absorption spectrum of EB−DNA is also changed with increasing r as shown in Figure 6.

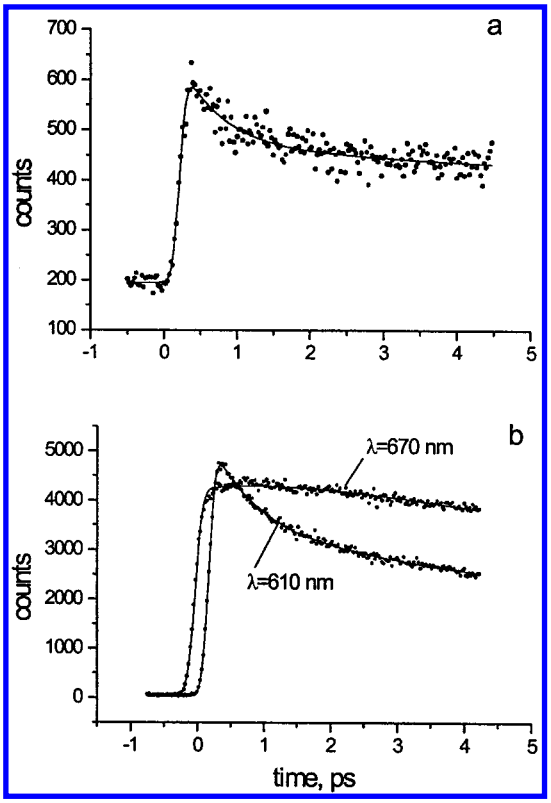

Figure 4. Fluorescence decays of EB−DNA and EB in water: (a) EB−DNA, $r = 0.3$, $\lambda_{em} = 580$ nm, fit: 600 fs − 40%; (b) EB in water, $\lambda_{em} = 610$ nm, fit: 700 fs 35%; $\lambda_{em} = 670$ nm, fit: rise 350 fs 13%.

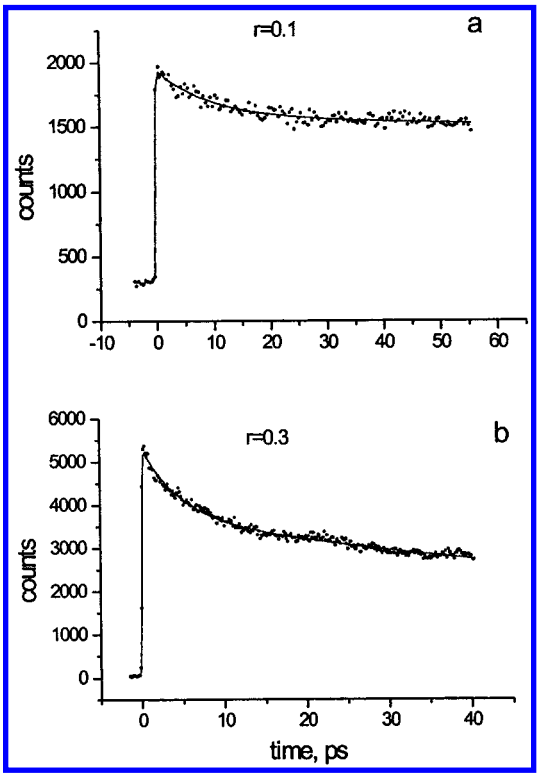

Figure 5. Fluorescence decay of AO−DNA, $\lambda_{em} = 550$ nm: (a) $r = 0.1$, fit: 10 ps 23%; (b) $r = 0.3$, fit: 5 ps 30%.

The same figure shows the spectrum for EB in glycerol solution (curve 4). The nonpolar environment simulates the environment of the dye in DNA stack. Note that the absorption and fluorescence spectra of EB in glycerol are very similar to that of EB intercalated into DNA. As can be seen, the transient

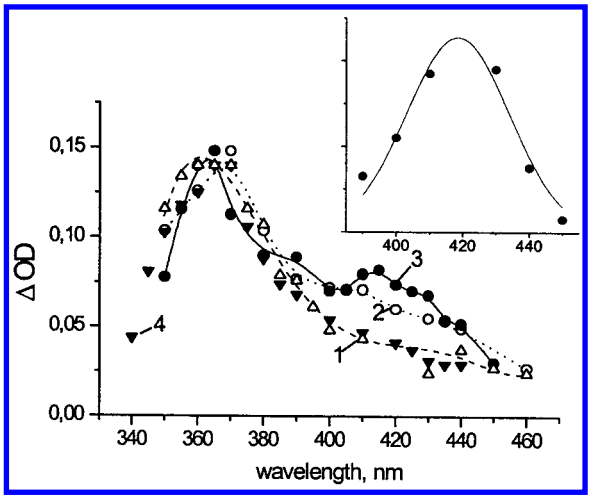

Figure 6. "In-pulse" transient absorption spectra of EB in glycerol solution and EB−DNA in aqueous solution during excitation with 532 nm laser pulse (20 ns): $r = 0.05$ (1), $r = 0.2$ (2), $r = 0.3$ (3); EB in glycerol (4). Inset: the difference of (3) and (1).

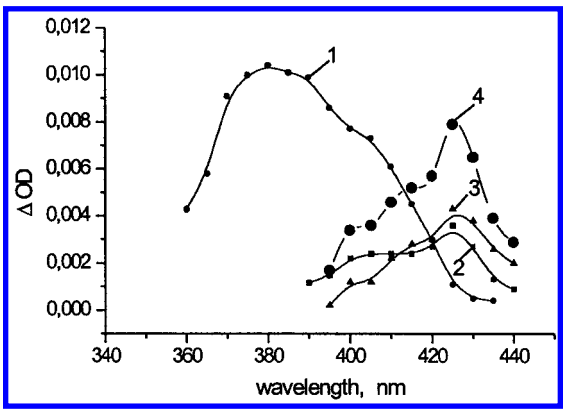

Figure 7. Transient absorption spectra of the species obtained after fitting of the decay curves of EB−DNA solution at $r = 0.3$ recorded on microsecond time scale: (1) species with lifetime $\tau = 84$ μs, (2) species with $\tau = 1.6$ μs, (3) species with $\tau = 1000$ μs, (4) the sum of the curves 2 and 3.

spectrum of EB in glycerol may be considered of as coinciding with that of EB−DNA at low r values. The spectrum obtained in aqueous solution appeared to be 5 nm blue-shifted relative to that for glycerol solution. Because of short lifetime of the transient signals, the signal-to-noise ratio is rather poor and this spectrum is not presented. The difference of the spectra at $r = 0.3$ and 0.05 is also shown in Figure 6 (insert). The decay curves recorded at $r = 0.3$ in the microsecond time scale appeared to be complex and dependent on the wavelength. A 3-exponential global fitting was applied to achieve reasonable data approximation. The component with the lifetime of 84 μs (curve 1 in Figure 7) has maximum at 390 nm and corresponds in spectrum to that of the triplet state of EB.[23] Two other components (curves 2, 3 in Figure 7), with $\tau_1 = 1.6$ μs and $\tau_2 \gg 100$ μs, exhibit the spectra with maximum at about 420 nm, which correspond to the spectrum of oxidized EB (EB^+).[11,23] The difference of the spectra at $r = 0.3$ and 0.05 obtained in nanosecond time scale (curve 5 in Figure 6) is also very close to the spectrum of EB^+. In the study of EB−DNA complex at lower r value, the oxidized EB was also observed, but it was formed in millisecond time scale and was assigned to a reaction of the triplet state with oxygen.[23] That is not the case for the oxidized EB observed in faster time scale. The results of flash photolysis study indicate, therefore, that electron transfer from the excited EB (EB*) is

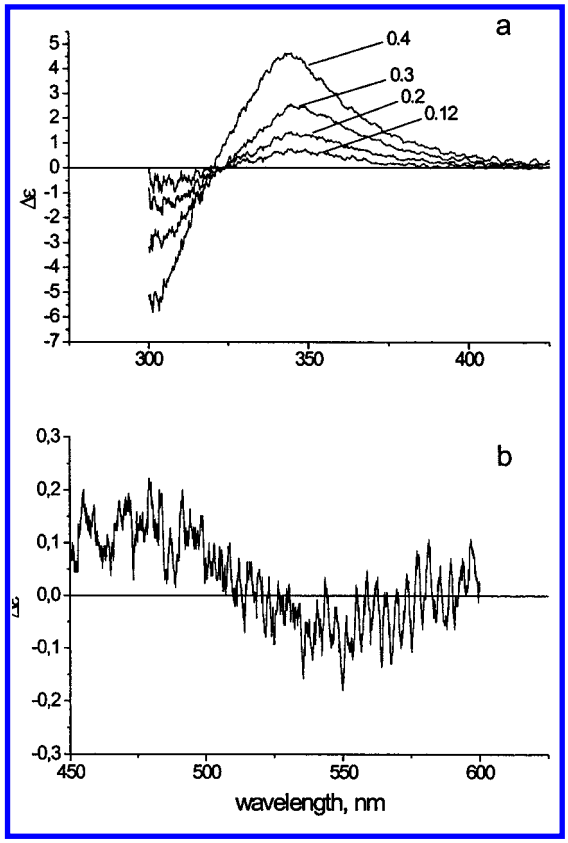

Figure 8. CD spectra of EB−DNA solution after subtraction of the limiting spectrum at $r = 0.03$: (a) the short-wave spectral region (the values of r are indicated); (b) the long-wave part of the spectrum at $r = 0.3$.

responsible for the fluorescence quenching. From the calculated values of the extinctions of EB^+ ($\epsilon = 1.7 \times 10^4$ M^{-1} cm^{-1} at 420 nm) and EB* ($\epsilon = 4.6 \times 10^3$ M^{-1} cm^{-1} at 370 nm),[23] one can estimate the relative amount of EB^+ to be ~10% in the nanosecond time domain and ~1% in the microsecond time domain at $r = 0.3$.

We have also studied the dependence of the CD spectrum of EB−DNA on r. CD spectrum is a very sensitive tool to reveal exciton interactions of the close-spaced chromophores. Figure 8 presents the difference spectra obtained after subtraction of the spectrum obtained at $r = 0.03$. After subtraction, only the exciton interaction of the dye contributes to the spectra. Indeed, the characteristic "conservative" exciton spectrum is evident in the short-wavelength region (Figure 8a). It is seen also in the range of the longer wavelength band at 530 nm (Figure 8b). The CD signal observed around 530 nm is essentially smaller than that at 350 nm. Hence, the exciton splitting of this band is probably less pronounced than that of high-energy transition. This can be due to smaller extinction of the longer wavelength band as compared to that of shorter one. The CD spectra at ionic strengths 0.1 and 0.001 showed similar dependencies on r, and the isosbestic point in the CD and absorption spectra persists at those ionic strengths. These facts allow one to state that possible aggregation of the dye on DNA surface does not contribute to the results obtained.

The transient absorption time-resolved spectra for the AO−DNA complex and AO in EtOH−H_2O solution were obtained on femtosecond time scale using pump−probe technique. Alcohol−water solution was used to avoid aggregation of the molecules. The spectra were recorded with the steps of 75 fs up to 1 ps delay and then with progressive steps up to 100 ps. The fitting procedure results in the spectra of components shown

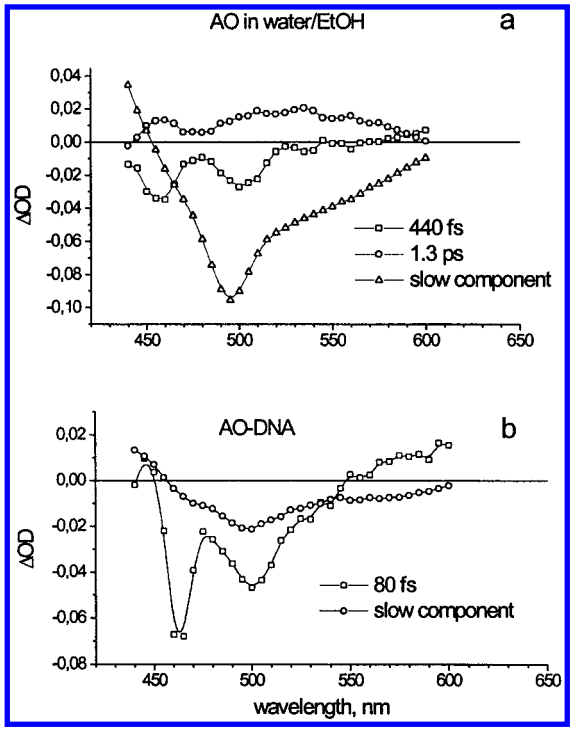

Figure 9. Transient absorption decay component spectra obtained after fitting procedure described in the Experimental Section: (b) AO−DNA in aqueous solution and (a) AO in EtOH/H_2O mixture (1:1, v). The decay time of the fast components is indicated. The slow components are practically constant within the time scale used (0−150 ps).

in Figure 9. A fast component of 80 fs in the AO−DNA case is very close in shape to a component of 440 fs obtained for AO in solution. The slow components (being practically constant in 100 ps time scale) can be assigned to thermally equilibrated relaxed excited state of AO. The multicomponent character of the spectra obviously reflects the evolution of the excited-state absorption during vibronic relaxation within $\approx 10^{-13}$ s. It should be noted that the ratio of the amplitudes of the components is quite different for the AO−DNA and AO−solution systems. This fact will be discussed in the following section.

Discussion

The fluorescence decay curves obtained for the EB−DNA and AO−DNA complexes reveal a fast component in picosecond time scale suggesting fluorescence quenching. The triplet state formation, as a possible reason for the fluorescence decay in picosecond time domain, may be disregarded because of low quantum yield of that process (∼0.1%[23]). The quenching time constant remains almost independent of r (Table 3), thus ruling out exciton dynamics as a possible explanation of the observations. It is interesting to note that the rate of electron transfer between azaguanine and excited EB in the DNA duplexes exhibited the same value of about 10 ps.[6] It appears that the fluorescence quantum yield of intercalated EB, φ, depends on the excitation wavelength: at 400 nm excitation φ is 2 times smaller (at the binding ratio $r = 0.3$) than that at 350 and 500 nm. This fact points at the heterogeneity of the EB−DNA complex. Obviously, there are a number of sites in the DNA structure which are responsible for the quenching, and the relative extinction coefficient at 400 nm for the EB molecules intercalated at those sites is higher than that for the other EB molecules. The fraction quenched in the picosecond time domain at $r = 0.3$ is increased significantly as compared with that at $r = 0.1$, as can be seen from the corresponding increase in the fractional amplitude of the fast component of the fluorescence decay curves obtained with the up-conversion method (Table 3). Similar result is observed for the AO−DNA complex (Figure 5). For the EB case, however, at $r > 0.3$, the fraction quenched in picosecond time scale decreases (Table 3). The variations in amplitude of the fast component of the fluorescence decay curves may be caused by a change in the relative extinction of the quenched fraction and/or by possible very effective energy migration between the nearest-neighboring dyes. Such domains of intercalated dyes in the DNA strand may be considered as linear aggregates of dyes being at the distance of approximately 10 Å. With increasing r, the size of such aggregates also increases. The factors mentioned above may act in opposite directions. That might lead to the nonmonotonic dependence on r in the EB case. Excitonic interactions between the nearest-neighboring dyes may account for both the change in extinction and in the efficiency of energy transfer. Those interactions are hardly seen in the region nearby the maxima of the absorption and luminescence spectra. The red tail in the absorption spectrum (curve 3 in Figure 1) and the corresponding 5 nm shift in the fluorescence (curve 6 in Figure 1) observed at high r might be considered as a weak manifestation of the exciton splitting. It appears, however, that excitonic interaction is clearly seen in the CD spectra (Figure 8) as a rise of the excitonic part of the CD signal. Excitonic interaction means delocalization of the electronic excitation over the neighboring dyes, which manifests itself as anomalously high bleaching of the ground-state absorption in the transient absorption spectra in femtosecond time domain.

The pump−probe experiments performed with AO−DNA complex and AO in solution resulted in transient absorption species shown in Figure 9. We have calculated the ratio of bleaching of the ground state absorption just after excitation (the sum of the amplitudes of the components) to that at a long delay time (the amplitude of the slow component) at the absorption maximum (500 nm). In the AO−DNA case, this value appears to be 3.5, while for the AO solution it is about 1. This fact is hardly explained by the possible inaccuracy of the fitting limited by the instrument time resolution (170 fs). The shorter lifetime might lead to underestimation of the amplitude. However, the lifetime of the fast component calculated in the AO−DNA case (80 fs) is shorter than that for the AO case (440 fs). Nevertheless, the relative amplitude of the fast component for AO−DNA complex appears to be much higher than that for AO solution. The above trivial explanation would lead to the opposite result. Strong bleaching of the ground state absorption of AO−DNA complex most likely results from the delocalization of the excitation in the Frank−Condon state over several (3−4) intercalated dyes followed by a fast (∼100 fs) localization. The same effect of the strong bleaching was observed for the antenna of purple photosynthetic bacteria and was explained by exciton delocalization over all core antenna bacteriochlorophylls.[28]

The fractions of EB and AO quenched in nanosecond time scale grow with increasing r, which is seen from a decrease in τ (Tables 1 and 2). This fact can be explained by the efficient energy migration to quenching sites by Forster mechanism that takes place at high r as was deduced from a decrease in the degree of fluorescence polarization.[18]

The transient absorption spectra obtained after excitation at 532 nm with 20 ns laser pulse reveal a small amount of oxidized EB: ∼1% in microsecond and ∼10% in nanosecond time scales. This indicates that the formation of oxidized EB is responsible for the fluorescence quenching.[29] The question arises: what is

the recipient of electron? EB in solution exhibits no picosecond component in the fluorescence quenching. The quenching of EB in solution results from the abstraction of proton of excited ethidium by the hydroxyl ion which takes place in nanosecond time scale.[30] The upper limit of oxidation potential of the excited EB is estimated as ~ -0.9 eV.[8] Hence, the reduction potential of the quenching sites should be higher than that value. DNA bases in solution do not possess such electron affinic properties. For example, cytosine and thymine bases, as most electron affinic, give the value -1.09 eV.[13] However, stacking might alter redox properties of the bases. Kononov and Bukina[16] have shown that there are sites with electronic levels lowered by about 1 eV in the synthetic polynucleotide poly(A). It was proposed that a specific stacking structure with a slight overlapping of electronic orbitals of the neighboring bases may result in charge-resonance (electron exchange) coupling.[16] Such sites with low-lying electronic levels might serve as electron acceptor in the EB−DNA system. On the other hand, similar electronic levels lying nearby the electronic levels of the donor and acceptor (dashed line in Scheme 1) can contribute significantly to the donor−acceptor coupling. In this case the system is characterized by a low difference in the energies of donor, bridge, and acceptor orbitals. As theory predicts,[15] distance dependence of the rate of electron tunneling becomes complex and cannot be reduced to an ordinary donor−bridge−acceptor system. The availability of such sites with electron exchange interactions, which might possess strong electron mobility, is likely dictated by the local structure of the DNA strand. It is not surprising then that if DNA with low amount of such regions per unit of length is used, they give no significant contribution to the apparent electron-transfer process. However, if such sites are realized in some synthetic duplexes of short length, it can lead to the shallow distance dependence of charge transfer.

Acknowledgment. The work was supported by the Academy of Finland, the National Program on Material and Structure Research, by the Technology Development Centre the Nanotechnology Programme, and by the Nordic Scholarship Scheme for the Baltic Countries and Northwest Russia.

References and Notes

(1) For reviews and theoretical aspects see, for example: (a) Netzel, T. J. *Chem. Educ.* **1997**, *74*, 646. (b) Beratan, D. N.; Priyadarshy, S.; Risser, S. M. *Chem. Biol.* **1997**, *4*, 3. (c) Jortner, J.; Bixon, M.; Langenbacher, T.; Michel-Beyerle, M. E. *Proc. Natl. Acad. Sci. U.S.A.* **1998**, *95*, 12759.

(2) Hall, D. B.; Holmlin, R. E.; Barton, J. K. *Nature* **1996**, *382*, 731. Nunez, M.; Hall, D. B.; Barton, J. K. *Chem. Biol.* **1999**, *6*, 85.

(3) (a) Gasper, S. M.; Schuster, G. B. *J. Am. Chem. Soc.* **1997**, *119*, 12762. (b) Henderson, P. T.; Jones, D.; Hampikian, G.; Kan, Y.; Schuster, G. B. *Proc. Natl. Acad. Sci. U.S.A.* **1999**, *96*, 8353.

(4) Dandliker, P. J.; Holmlin, R. E.; Barton, J. K. *Science* **1997**, *275*, 1465.

(5) Meggers, E.; Michel-Beyerle, M. E.; Giese, B. *J. Am. Chem. Soc.* **1998**, *120*, 12950.

(6) Wan, C.; Fiebig, T.; Kelley, S. O.; Treadway, C. R.; Barton, J. K.; Zewail, A. H. *Proc. Natl. Acad. Sci. U.S.A.* **1999**, *96*, 6014.

(7) Murphy, C. J.; Arkin, M. R.; Jenkins, Y.; Ghatlia, N. D.; Bossmann, S. H.; Turro, N. J.; Barton, J. K. *Science* **1993**, *262*, 1025.

(8) Kelley, S. O.; Holmlin, R. E.; Stemp, E. D. A.; Barton, J. K. *J. Am. Chem. Soc.* **1997**, *119*, 9861.

(9) Murphy, C. J.; Arkin, M. R.; Ghatlia, N. D.; Bossmann, S. H.; Turro, N. J.; Barton, J. K. *Proc. Natl. Acad. Sci. U.S.A.* **1994**, *91*, 5315. Arkin, M. R.; Stemp, E. D. A.; Holmlin, R. E.; Barton, J. K.; Hörmann, A.; Olson, E. J. C.; Barbara, P. F. *Science* **1996**, *273*, 475.

(10) Lincoln, P.; Tuite, E.; Nordén, B. *J. Am. Chem. Soc.* **1997**, *119*, 1454. Olson, E. J. C.; Hu, D.; Hörmann, A.; Barbara, P. F. *J. Phys. Chem. B* **1997**, *101*, 299.

(11) (a) Brun, A. M.; Harriman, A. *J. Am. Chem. Soc.* **1992**, *114*, 3656. (b) Atherton, S. J.; Beaumont, P. C. *J. Phys. Chem.* **1995**, *99*, 12025.

(12) Priyadarshy, S.; Risser, S. M.; Beratan, D. N. *J. Phys. Chem.* **1996**, *100*, 17678.

(13) Steenken, C.; Telo, J. P.; Novais, H. M.; Candeias, L. P. *J. Am. Chem. Soc.* **1992**, *114*, 4701. Note that the redox potentials for the bases in aprotic solvent even shift negatively by ca. 1 eV: Seidel, C. *Proc. SPIE: Biomol. Spectrosc. II*, **1991**, *1432*, 91.

(14) Newton, M. D.; Sutin, N. *Annu. Rev. Phys. Chem.* **1984**, *35*, 437. Marcus, R. A.; Sutin, N. *Biochim. Biophys. Acta* **1985**, *811*, 265. Jortner, J. *J. Chem. Phys. Chem.* **1976**, *64*, 4860.

(15) Evenson, J. W.; Karplus, M. *Science* **1993**, *262*, 1247.

(16) Kononov, A. I.; Bukina, M. N. *Book of Abstracts*, XVIII-th International Conference on Photochemistry, Warsaw, August 3−8, 1997; p 329. Kononov, A. I.; Bukina, M. N. *J. Photochem. Photobiol. B: Biol.*, in press.

(17) Förster, T. *Discuss. Faraday* **1959**, *27*, 7.

(18) Baguley, B. C.; Bret, M. L. *Biochemistry* **1984**, *23*, 937.

(19) Dalgleish, D. G.; Fujita, H.; Peacocke, A. R. *Biopolymers* **1969**, *8*, 633. Houssier, C.; Hardy, B.; Fredericq, F. *Biopolymers* **1974**, *13*, 1141; Volkenstein, M. V. *Mol. Biol.* **1977**, *11*, 917 (in Russian).

(20) (a) Tkachenko, N. V.; Grandell, D.; Ikonen, M.; Jutila, A.; Moritz, V.; Lemmetyinen, H. *Photochem. Photobiol.*, **1993**, *58*, 284. (b) Tkachenko, N. V.; Rantala, L.; Tauber, A. Y.; Helaja, J.; Hynninen, P. H.; Lemmetyinen, H. *J. Am. Chem. Soc.* **1999**, *121*, 9378.

(21) Waring, M. J. *J. Mol. Biol.* **1965**, *14*, 269. LePecq, J.-B.; Paoletti, C. J. *J. Mol. Biol.* **1967**, *27*, 87. Pauluhn, J.; Gaugain, B.; Barbet, J.; Capelle, N.; Roques, B. P.; LePecq, J.-B. *Biochemistry* **1978**, *17*, 5078.

(22) Atherton, S. J.; Beaumont, P. C. *Photochem. Photobiol.* **1986**, *44*, 103.

(23) Atherton, S. J.; Beaumont, P. C. *J. Phys. Chem.* **1987**, *91*, 3993.

(24) Fiebig, T.; Wan, C.; Kelley, S. O.; Barton, J. K.; Zewail, A. H. *Proc. Natl. Acad. Sci. U.S.A.* **1999**, *96*, 1187.

(25) Olmsted, J.; Kearns, D. R. *Biochemistry* **1977**, *16*, 3647.

(26) Fredericq, F.; Houssier, C. *Biopolymers* **1970**, *9*, 639; **1972**, *11*, 2281.

(27) Brun, A. M.; Harriman, A. *J. Am. Chem. Soc.* **1994**, *116*, 10383.

(28) Novoderezhkin, V. I.; Razjivin, A. P. *FEBS Lett.* **1993**, *330*, 5. Novoderezhkin, V. I.; Razjivin, A. P. *FEBS Lett.* **1994**, *345*, 203. Novoderezhkin, V. I.; Razjivin, A. P. *Biophys. J.* **1995**, *68*, 1089. Novoderezhkin, V. I.; Razjivin, A. P. *Biofizika* **1997**, *42*, 164.

(29) It should be noted that the oxidized EB observed in the flash photolysis experiments is not direct proof that the electron transfer occurred in the picosecond time domain. In this respect, the electron-transfer products observed in the pump−probe experiments would be more convincing. Unfortunately, the setup used in this study (the excitation is at 400 nm) did not allow us to perform such measurements.

(30) Ohmstead, J., III; Kearns, D. R. *Biochemistry* **1977**, *16*, 3647. Pal, S. K.; Mandal, D.; Bhattacharyya, K. *J. Phys. Chem. B* **1998**, *102*, 11017.